Title
Pit and rim formation during laser marking of acrylonitrile butadiene styrene plastic

Journal
Journal of Laser Applications, 17(4)

ISSN
1042-346X

Authors
Shin, Yongjin
Kim, Youngseop
Park, Sohee
et al.

Publication Date
2005-11-01

DOI
10.2351/1.2080405

Pit and rim formation during laser marking of acrylonitrile butadiene styrene plastic

Yongjin Shin[a)]
Department of Physics, Chosun University, Gwangju 501-759, South Korea and Beckman Laser Institute, University of California at Irvine, Irvine, California 92612

Youngseop Kim and Sohee Park
Laser Imaging Laboratory, Chosun University, Gwangju 501-759, South Korea

Byungjo Jung
Department of Biomedical Engineering, Yonsei University, Wonju 220–710, South Korea

Jangwoen Lee[b)] and J. Stuart Nelson
Beckman Laser Institute, University of California at Irvine, Irvine, California 92612

(Received 11 August 2004; accepted for publication 14 April 2005)

Pit and rim formation on the acrylonitrile butadiene styrene (ABS) plastic surface was evaluated after it was irradiated by CO_2 and Nd:yttrium-aluminum-garnet (YAG) laser beams. Our results show that the thermal effect floor was well observed at the outer wall of the pit with CO_2 laser irradiation while it was not the case with Nd:YAG laser irradiation. The volume and depth of the pit formation increase proportionally with laser irradiation energy while there are significant differences in the slope, width, and full width at half maximum of the pit formation with two different types of laser irradiations. This result shows that CO_2 laser irradiation leads to a better cooling contraction effect while Nd:YAG laser irradiation induces a better recoil pressure effect during the interaction between ABS plastic and laser beam irradiation. The shape of the laser marking could vary significantly depending on the traveling path of molten plastic during injection molding of ABS plastic. Therefore, the selection of material and molding process can have a great impact on the laser micromachining of plastic.

Key words: pit and rim formation, laser marking, heat flow, mass motion

I. INTRODUCTION

Light amplification by stimulated emission of radiation is currently used as an innovating technology in industry, science, medicine, and military. Especially, high power CO_2 and Nd:yttrium-aluminum-garnet (YAG) lasers have been rapidly replacing conventional processing methods recently.[1] The requirements for hyperprecision processing due to the device miniaturization have accelerated advances in laser processing technology.[2,3]

These advances in laser processing technology have lead to a wide range of research on physical and chemical interactions between laser and material. As a result, laser marking methods utilizing the modification effect on thin film have been proposed recently.[4–6] Also micromachining systems using laser marking on plastic have been pursued in recent research because plastic has greater thermal and electrical resistance and has a higher tolerance against breaking when compared to metal.[7–9] Despite apparent advantages in using plastic as a processing material, the modification effect and laser interaction with plastic have only been predicted indirectly by a numerical analysis, and direct measurements of modified shapes have not been available. In addition, further research is necessary to understand material characteristics and processing phenomena fundamentally.

In this article, we investigated physical changes and shape modification during pit formation in order to understand laser marking mechanism on the acrylonitrile butadiene styrene (ABS) plastic surface macroscopically after CO_2 and Nd:YAG laser beam irradiation. As a result, the practical issues of hyperprecision laser processing on plastic can be addressed from this experiment.

II. BACKGROUND

Laser spot marking is the formation of a small pit using a highly focused laser beam and it generally involves three physical processes: optical absorption, heat flow, and mass motion. Upon a short temporal irradiation of the laser beam, a portion of the irradiated energy is spontaneously absorbed according to reflexibility of the material.

Absorbed laser beam energy acts as a thermal source and the following melting process causes heat flow around the irradiated area. As a result, the surface of the pit center caves in and the bulge is formed at the periphery of the pit. The formation of the bulge results from the blackbody radiation of the "keyhole" formation by the collapsed surface. The proportion of the absorbed laser beam energy is reradiated

[a)]Electronic mail: yjshin@chosun.ac.kr and yshin@laser.bli.uci.edu
[b)]Electronic mail: jangwl@uci.edu

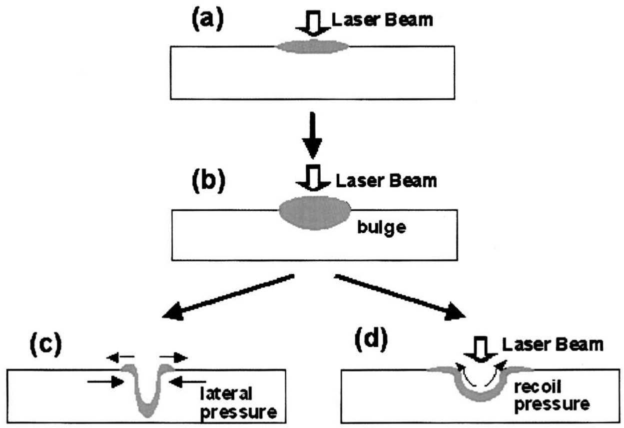

FIG. 1. Schema of proposed mechanism: (a) molten bulge produced by local thermal expansion, (b) flow of bulge caused by surface tension, (c) forming of rim by contraction upon cooling, and (d) forming of rim by recoil pressure.

outward, while the rest is transferred inside the material as heat flow causing morphological changes of the material. Absorbed laser beam energy decreases spontaneously at the keyhole-shaped pit. The exponential decrease of the energy follows the Lambert-Beer law, or $I=I_0e^{(-\alpha d)}$, where I_0, α, and d are the irradiated beam intensity, absorption coefficient, and depth, respectively.[10] Due to the heat flow from the optical absorption, the pit and rim are formed on the material surface. The formation of the pit and rim can be explained by two major mechanisms, contraction upon cooling and recoil pressure.

At first, during the laser marking process, the surface tension from the temperature gradient drives flow of melted material, and the pit and rim are created by the contraction of melted material during the cooling process. The protrusion of material can be explained by the series of processes, which include volume changes from the heat flow and surface contraction during cooling.[11,12] Because these processes occur in a relatively short time period, experimental investigation is rather difficult and only the numerical approximation of processes was possible. Figures 1(a)–1(c) show the schematic sequence of the proposed pit and rim formation by the cooling contraction.

Recoil pressure is the second mechanism for the rim formation. The viscosity of material induces a short temporal ablation at high temperature. It also causes a volume decrease and material decomposition, which, in turn, initiates the mass motion. Therefore, viscosity induced ablation forms the pit and rim via recoil pressure. A series of pit and rim formation processes occurs almost simultaneously. A sudden temperature increase from the laser beam irradiation causes ablation during material recomposition. The recoil pressure from ablation pushes the mass motion toward the surface and away from the lateral pressure, and creates the rim. As irradiation energy of the laser beam increases, the molten layer becomes thinner. Consequently, recoil pressure decreases gradually.[13,14] The rim formation mechanism involving recoil pressure is illustrated sequentially in Figs. 1(a), 1(b), and 1(d).

TABLE I. Physical properties of ABS plastic.

Classification	Value
Density (g/cm^3)	1.04–1.06
Tensile strength (N/mm^2)	32–45
Thermal conductivity (W/mK)	0.18
Thermal diffusivity (10^{-3} cm^2/s)	1.4
Specific heat (kJ/kg K)	1.3
Hardness	85–97
Heat deflection temp. (°C)	95–110
Coefficient of linear expansion ($K^{-1}10^6$)	60–110
Surface tension (dyn/cm)	<40
Viscosity (poise)	>1

III. EXPERIMENTS

A CO_2 laser ($\lambda=10.64$ μm) with the average output power of 13 W was used for the experiment while operating in pulse width modulation mode. It has the output beam diameter of 3 mm and the beam divergence of 4 mR. The output beam from the resonator first passes through the beam expander (2.7 folds), and is incident upon a ZnSe-coated *X-Y* galvanometer scan mirror. Finally, the reflected laser beam from the mirror is focused by the planoconvex f-θ lens ($f=154.2$ mm). On the other hand, a *Q*-switched mode Nd:YAG laser ($\lambda=1.064$ μm) has the output power of 80 and 20 W at multimode and TEM_{00} mode, respectively. The beam diameters for multi and TEM_{00} modes are 4 and 1.2 mm, respectively, and the beam divergences are 6 and 2.5 mR for each mode. As with the CO_2 laser, a 2.7 fold-beam expander, a ZnSe-coated *X-Y* galvanometer scan mirror and 225 mm focal length ZnSe planoconvex f-θ lens were used for the irradiation of the laser beam. The incident energy of both a CO_2 and Nd:YAG laser ranges between 30 and 1000 mJ. The minimum incident energies of respective lasers were determined at the lowest possible energy level to produce the observable laser spot marking on the sample.

A microscope (Dongwan, OSM-1) with 40× and 80× magnifications was used to observe the surface and cross section of the pit and rim created by the laser beam incident on the sample. To avoid possible defects on the cross section of a laser marking area and to minimize the sample collapse due to the ductility of plastic, samples were snap frozen to −200 °C with pure liquid nitrogen and were cut by applying the sudden force on a symmetrical plane around the center of pit. A digital image analysis program was used to investigate the cross-sectional view of the pit, rim, and thermal effect floor of the laser marking. The final images were obtained using a 60× magnification. The digital image of the cross section was projected onto the transparent grid film (1 mm scale) to acquire a relative coordination of the cross section of the sample. The shape of the cross section was approximated as a Gaussian function based on the acquired relative coordination.

We prepared ABS plastic samples (50×20×2 mm) from common ABS resin (LG AF-302) using an injection molding technique. Physical properties of ABS plastic samples are listed in Table I. We used the injection molding ABS plastic as a sample because it is not only tolerant

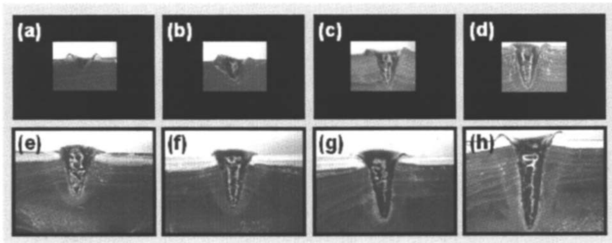

FIG. 2. The cross-sectional view of ABS plastic after CO_2 laser irradiation; (a) 50, (b) 100, (c) 200, (d) 300, (e) 400, (f) 500, (g) 750, and (h) 1000 mJ; 60× magnification.

against breaking but also has a higher thermal and electrical resistance compared to ceramic, glass, or metal. In addition, ABS plastic is easy to process.

IV. RESULTS AND DISCUSSIONS

Figures 2 and 3 show the cross-sectional view of the laser marking and the pit/rim shapes after CO_2 and Nd:YAG laser irradiations, respectively. Figure 2 clearly shows the thermal effect floor formation around the pit. The thermal effect floor is distributed symmetrically around the pit and pictures show that the ratio between the width and depth of the pit increases as irradiation energy increases. Contrary to CO_2 laser beam marking, the thermal layer was not observed in Nd:YAG laser marking (Fig. 3), and the increase of the ratio between the width and depth of the pit was relatively small with the irradiation energy increase.

Because the simultaneous formation of the pit and rim occurs spontaneously only the numerical approximation of the proposed processes shown in Fig. 1 has been possible. However, Figs. 2 and 3 show that it is possible to experimetally observe and separate the processes due to contraction upon cooling and recoil pressure during the pit/rim formation.

Changes in depth, width, and full width at half maximum (FWHM) are plotted as a function of the irradiation energy in Fig. 4. In CO_2 laser irradiation, the depth of the pit increased linearly ($1.6\ \mu m/mJ$) with the energy, while the increase in width was less conspicuous. The rate of the increase in the width slowed down after 400 mJ. The progression of the FWHM was similar ($\sim 370\ \mu m$) to the width, and it reached its maximum at 500 mJ. Changes in depth, width, and FWHM of the pit with Nd:YAG laser irradiation were similar to CO_2 laser irradiation. The depth increased linearly

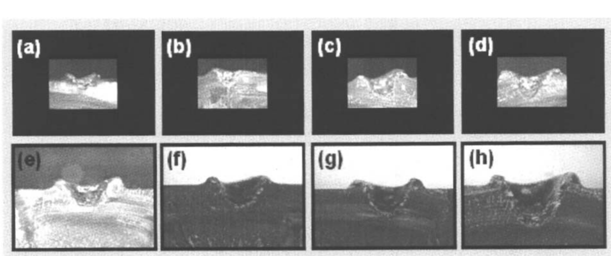

FIG. 3. The cross-sectional view of ABS plastic after Nd:YAG laser irradiation; (a) 50, (b) 100, (c) 200, (d) 300, (e) 400, (f) 500, (g) 750, and (h) 1000 mJ; 60× magnification.

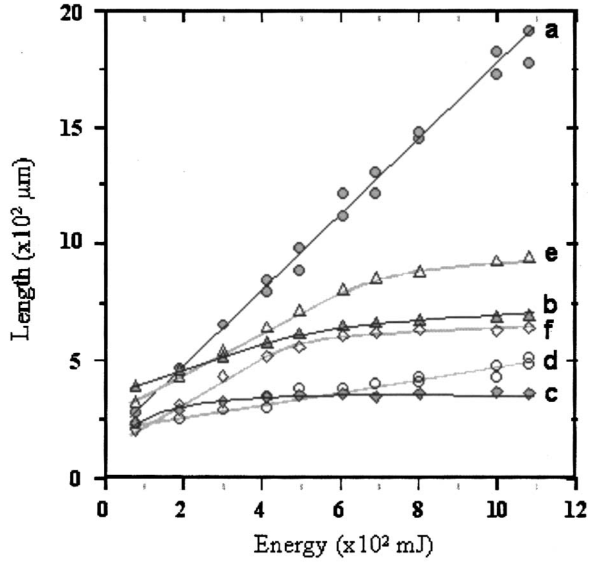

FIG. 4. Changes in depth, width, and FWHM with CO_2 and Nd:YAG laser irradiations; (a) CO_2—depth, (b) CO_2—width, (c) CO_2—FWHM, (d) Nd:YAG—depth, (e) Nd:YAG—width, and (f) Nd:YAG—FWHM.

($0.6\ \mu m/mJ$) with the irradiation energy. The width increased linearly up to 600 mJ and its rate of increase slowed down at a higher energy level. The increase of the FWHM was also linear up to 400 mJ, but the rate of the increase slowed down afterward reaching its maximum ($630\ \mu m$) at 700 mJ.

The pit volume is also plotted as a function of the irradiation energy in Fig. 5. With both CO_2 and Nd:YAG laser irradiations, the pit volume increased linearly. However, there was a significant difference in slopes with two types of irradiation ($19.4 \times 10^4\ \mu m^3/mJ$ for CO_2 and $9.5 \times 10^4\ \mu m^3/mJ$ for Nd:YAG laser irradiations, respectively).

From the results from Figs. 4 and 5, we concluded that the CO_2 laser with its longer wavelength exerts better cooling contraction effects since the laser energy mostly contrib-

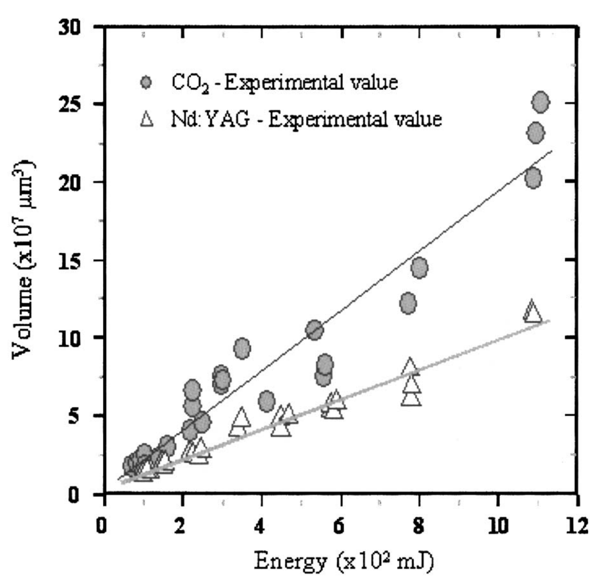

FIG. 5. The changes of pit volume with CO_2 and Nd:YAG laser irradiation.

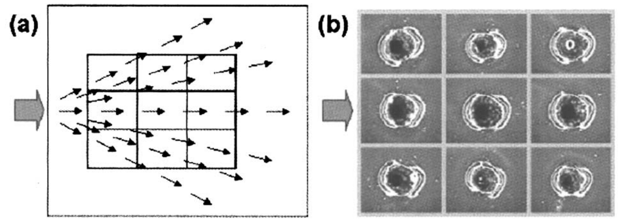

FIG. 6. Photography of laser spot marking on the surface of ABS plastic; (a) traveling course of molten plastic in an injection mold, (b) rim's orientation by laser spot marking corresponding to the injection direction.

utes to the volume change from the heat flow and resulted in the deep pit formation. On the other hand, compared to CO_2 laser irradiation the rates of increase in the depth and volume were slower 2.67 and 2.04 folds, respectively, with shorter-wavelength Nd:YAG laser irradiation.

During the pit formation due to recoil pressure, the volume change is caused by the viscosity induced ablation. However, the presence of recoil pressure favors the mass motion toward the surface and causes the formation of a shallower pit compared to those from the heat flow. These experimental results and characteristics of the pit shapes lead us to coclude that a Nd:YAG laser with a shorter wavelength exerts better a recoil pressure effect on ABS plastic.

Figure 6 shows the surface profiles of the rim during the pit formation by laser irradiations. Because ABS plastic samples were prepared by the injection molding, viscous flow of ABS resin exists inside the injection mold during fabrication. The direction of viscous flow gives rise to a direction of mass motion and a subsequent rim orientation. The prescribed direction of viscous flow also explains the asymmetry of rim formation in Fig. 6. When molten plastic resin is injected through a small nozzle of the mold, the pressure difference at the nozzle creates a turbulent flow of molten resin, and the turbulence results in the different orientation of the rims. This different orientation of the rims should not be overlooked because the shape and size of the rim play an important role in micromachining (marking, drilling, cutting, engraving) of plastic as well as those of the pit.

V. CONCLUSIONS

We observed the formation of the pit and rim on the ABS plastic surface by CO_2 and Nd:YAG laser irradiations and investigated the interaction between ABS plastic and laser irradiation energy and marking mechanisms. The volume and depth of the pit are nearly proportional to the irradiation energy and it shows a uniform proportion of absorbed energy was used for the pit formation.

Characteristics and shapes of the pits, especially slopes, differ with CO_2 and Nd:YAG laser irradiations. This fact implies a CO_2 laser with a longer wavelength ($\lambda = 10.64\ \mu m$) exerts a better cooling contraction effect on ABS plastic while a Nd:YAG laser with a shorter wavelength ($\lambda = 1.06\ \mu m$) induces a more effective recoil pressure.

In addition, we demonstrated the shape of the laser marking varies significantly depending on the direction of molten plastic during fabrication. Also, the fabrication method as well as the selection of material plays an importance role when plastic is used as a base material for the laser micromachining.

ACKNOWLEDGMENTS

This study was supported in part by research grants from Chosun University, South Korea.

[1]J. Wilson and J. F. B. Hawkes, *Laser Principles and Applications* (Prentice Hall, United Kingdom, 1987).
[2]R. R. Tummala and E. J. Rymaszeski, *Microelectronics Packaging Handbook* (Van Nostrand Reinhold, New York, 1989).
[3]Y. J. Shin and Y. G. Kang, "Laser micro-machining," J. Kor. Electric. Electro. Mater. Engin. **14**, 1–6 (2001).
[4]K. Y. Law and G. E. Johnson, "Ablative optical recording using organic dye-in-polymer thin films," J. Appl. Phys. **54**, 4799–4805 (1983).
[5]D. A. Hill and D. S. Soong, "A model for laser marking of thin organic data storage layers by short intense pulse," J. Appl. Phys. **61**, 2132–2135 (1987).
[6]K. F. Wissbrun, "Thermal expansion and flow model for pit formation in laser marking of polymeric film optical disks," J. Appl. Phys. **62**, 1123–1124 (1998).
[7]Y. M. Noor, S. C. Tam, L. E. N. Lim, and S. Jana, "A review of the Nd:YAG laser marking of plastic and ceramic IC packages," J. Mater. Process. Technol. **42**, 95–133 (1994).
[8]S. H. Slivinsky and N. E. Ogle, "Laser beam interaction with plastic," J. Appl. Phys. **48**, 3660–3664 (1977).
[9]J. H. Chang, Y. J. Shin, K. W. Jeong, J. H. Lee, and J. O. Kim, "Development of laser marking and drilling system for high speed moving object," J. Kor. Laser Tech. **101**, 51–55 (2002).
[10]M. Lax, "Temperature rise induced by a laser beam," J. Appl. Phys. **48**, 3919–3924 (1977).
[11]T. S. Chung, "Pit formation during laser marking of thin organic films," J. Appl. Phys. **60**, 55–60 (1986).
[12]K. F. Wissbrun, "Thermal expansion and flow model for pit formation in laser marking of polymeric film optical disks," J. Appl. Phys. **62**, 1123–1124 (1998).
[13]J. J. Wrobel, A. B. Marchant, and D. G. Howe, "Laser marking of thin organic films," Appl. Phys. Lett. **40**, 928–930 (1982).
[14]M. C. Gupta, "A study of laser marking of thin films," J. Mater. Res. **3**, 1187–1195 (1988).